Direct Observation of Nucleus Structure and Nucleation Pathways in Apoferritin Crystallization

S.-T. Yau[†] and Peter G. Vekilov*[,†,‡]

Contribution from the Department of Chemistry and the Center for Microgravity and Materials Research, University of Alabama in Huntsville, Huntsville, Alabama 35899

Received August 15, 2000

Abstract: Using atomic force microscopy (AFM) in situ during the crystallization of the protein apoferritin from its solution, we imaged the arrangement of the molecules in near-critical clusters, larger or smaller than the crystal nucleus, that are representative of the nucleus structure. At supersaturations $\Delta\mu/k_BT$ of 1.1 − 1.6 − 2.3, the nuclei contain about 50 − 20 − 10 molecules. The molecular arrangement within the nuclei is similar to that in the crystal bulk. Contrary to the general belief, the observed nuclei are not compact molecular clusters, but are planar arrays of several rods of 4−7 molecules set in one or two monomolecular layers. Similarly unexpected nuclei structures might be common, especially for anisotropic molecules. Hence, the nucleus structure should be considered as a variable by advanced theoretical treatments.

Introduction

The central problem of nucleation theory and experiment is that of determination of the nucleation rates as a function of the parameters controlling the process.[1,2] Some approaches to the solution of this problem concentrate on finding the dependence of the total surface free energy of the new-phase clusters Φ on the number of atoms or molecules in them n, $\Phi(n)$.[3,4] For a large spherical nucleus with radius r and surface energy γ, $\Phi = 4\pi r^2\gamma$. However, in many situations, the clusters are smaller than 100 atoms or molecules, γ is ill-defined, and the nucleus shape cannot be approximated with a sphere. Although often a compact three-dimensional arrangement of the molecules in the nucleus is assumed,[5,6] there is no direct experimental evidence of the nucleus shape and structure for any system. The problem is very intriguing: molecular dynamics simulations predict a compact nucleus structure for atoms or molecules with a spherical interaction field,[7,8] while strongly anisotropic, dipolar molecules may have a nucleus consisting of a single chain of molecules.[9] Furthermore, a recent theory, which accounts for the relaxation of the surface layer atoms or molecules in a cluster and its dependence on the thickness of the underlying crystalline matter, predicts, for some cases, planar critical clusters.[10]

The experimental difficulties in visualization of the structure of the critical clusters can be grouped into three categories: (a) the constituent atoms or molecules are so small that even if the clusters are detected, their structures cannot be discerned by most microscopic techniques; (b) the critical clusters exist for extremely short times after which they either grow to macroscopic crystals or decay; and (c) the critical clusters are relatively small, and due to Brownian diffusion, they freely move throughout the available volume of the mother phase.

The former two of these difficulties can be overcome by using a protein crystallization model system. The sizes of the protein molecules are a few nanometers,[11] and the typical times between sequential discrete growth events are a few seconds.[12] These sizes and time scales are within the reach of the modern atomic force microscopy (AFM) techniques.[13] A further advantage of AFM is that this method allows in situ, real-time, molecular-resolution monitoring of the processes of interest at room temperature and atmospheric pressures, i.e., at conditions under which protein crystallization typically occurs.[14−17]

However, as a surface characterization technique, atomic force microscopy (AFM) can be applied to visualize clusters that appear in the solution bulk only if they reach a surface and adsorb on it. We can evaluate the time τ required for a cluster formed within a distance $x = 100$ μm from the cell bottom to reach it through Brownian motion from Einstein's relation

* Address correspondence to this author.
† Center for Microgravity and Materials Research.
‡ Department of Chemistry.

(1) Oxtoby, D. W. *J. Phys.: Condens. Matter* **1992**, *4*, 7627−7650.
(2) Oxtoby, D. W. *Acc. Chem. Res.* **1998**, *31*, 91−97.
(3) Gibbs, J. W. *The Collected Works of J. W. Gibbs*; Yale University Press: New Haven, 1961; Vol. 1.
(4) Neilsen, A. E. In *Crystal Growth*; Peiser, S., Ed.; Pergamon: Oxford, 1967; pp 419−426.
(5) Milchev, A. *Contemp. Phys.* **1991**, *32*, 321−332.
(6) Chernov, A. A. *Modern Crystallography III: Growth of Crystals*; Springer: Berlin, 1984.
(7) ten Wolde, P. R.; Frenkel, D. *Science* **1997**, *277*, 1975−1978.
(8) Talanquer, V.; Oxtoby, D. W. *J. Chem. Phys.* **1998**, *109*, 223−227.
(9) ten Wolde, P. R.; Oxtoby, D. W.; Frenkel, D. *Phys. Rev. Lett.* **1998**, *81*, 3695−3698.
(10) Lee, W. T.; Salje, E. K. H.; Dove, M. T. *J. Phys.: Condens. Matter* **1999**, *11*, 7385−7410.
(11) Creighton, T. E. *Proteins: structure and molecular properties*; W. H. Freeman: New York, 1993.
(12) Yau, S.-T.; Thomas, B. R.; Vekilov, P. G. *Phys. Rev. Lett* **2000**, *85*, 353−356.
(13) Binnig, G.; Gerber, C.; Stoll, E.; Albrecht, R. T.; Quate, C. F. *Europhys. Lett* **1987**, *3*, 1281−1286.
(14) Yau, S.-T.; Petsev, D. N.; Thomas, B. R.; Vekilov, P. G. *J. Mol. Biol.* **2000**, *303*, 667−678.
(15) Land, T. A.; DeYoreo, J. J.; Lee, J. D. *Surf. Sci.* **1997**, *384*, 136−155.
(16) Malkin, A. J.; Kuznetsov, Y. G.; McPherson, A. *J. Cryst. Growth* **1999**, *196*, 471−488.
(17) Kuznetsov, Y. G.; Malkin, A. J.; Land, T. A.; DeYoreo, J. J.; Barba, A. P.; Konnert, J.; McPherson, A. *Biophys. J.* **1997**, *72*, 2357−2364.

10.1021/ja003039c CCC: $20.00
Published on Web 01/17/2001

$x^2 = 2D\tau$.[18] A lower estimate for cluster diffusivity D can be obtained from the diffusivity of single apoferritin molecules, 3.2×10^{-7} cm^2 s^{-1}, refs 19 and 20 using Stokes law and assuming that the clusters behave like particles with seven molecules (cluster size to be verified below) at an edge: $D \approx 5 \times 10^{-8}$ cm^2 s^{-1}. Substituting, we get $\tau \approx 1000$ s ≈ 15 min. (The times for sedimentation of particles whose density is only slightly higher than the solution density[21] in the Earth's gravity field, using the formula of ref 22, are longer by more than an order of magnitude.) Thus, in its random walk throughout the solution, a near-critical cluster may land on the cell bottom and, provided that the characteristic times of its existence are of the order of 15 min, we may be able to detect it and monitor its evolution.

The goal of the experiments discussed here was to image at molecular resolution, in situ in supersaturated solutions the subcritical, near-critical, and supercritical clusters for the crystallization of a model protein system as these clusters adsorb on the bottom of the AFM cell and gain insight into the nucleation pathways.

We used the protein apoferritin, whose molecules are the hollow shells of the iron-storage protein ferritin[23] and consist of 24 subunits arranged in pairs along the 12 walls of a quasi-rhombododecahedron.[24,25] Apoferritin crystals have a face-centered cubic (fcc) lattice and are faceted by [111] planes with a beehive arrangement of the molecules.[12,26] A brief account of some of the results presented here has been published in ref 27.

Experimental Section

Apoferritin was purified from commercial preparations (Sigma, St. Louis) as described in ref 26. Crystallizing solutions containing 0.02−0.25 mg·mL^{-1} of protein and 2.5% (w/v) $CdSO_4$ precipitant in a 0.05 M acetate buffer were prepared as described in refs 20 and 26. The supersaturation of the solution with respect to the crystalline phase was determined as $\sigma \equiv \Delta\mu/k_BT = \ln(\gamma\ C/\gamma_e C_e)$, where C and $C_e = 23$ μg·mL^{-1} are the actual and equilibrium protein concentrations. This C_e was determined as C at which the unfinished layers on the surface of a large crystal stopped spreading, before retreating in solutions of $C < C_e$. As shown in ref 14, at these low protein concentrations, the activity coefficients γ and $\gamma_e \approx 1$.

Monitoring of the nucleation and growth was carried out in situ in the AFM (Nanoscope IIIa, Digital Instruments, Santa Barbara, CA) fluid cell at 23.0 ± 0.3 °C, maintained by stabilizing the room temperature. This temperature was higher by 0.5−1 °C than the setting in the room. The insensitivity of apoferritin crystallization to temperature variations[26,28] justifies this approach to temperature stabilization. We employed the tapping mode imaging using SiN tips with a minimal force constant. This mode is less intrusive and allows visualization of adsorbed protein and impurity species (tip impact in the contact imaging mode often prevents such imaging).[29,30] The tapping frequency was around 30 kHz, depending on the resonance frequency of the specific cantilever used. Typical scanning frequencies were between 2 and 5 Hz, which allowed intervals between 256 scan line images of ~120−50 s. To shorten these intervals, in a few cases rectangular images, with a 2:1 ratio of the dimensions, consisting of 128 scan lines, were collected. The scanning parameters were adjusted such that continuous imaging affected neither the surface structure nor the process dynamics. For verification, we varied the scan sizes, the direction of scanning, and the time elapsed between image collections, and saw that neither the spatial nor the temporal characteristics of the monitored nucleation and growth processes changed; see also comments related to Figures 5−7 below. Details about the calibration, further tests, and determination of the maximum resolution of the method are provided in ref 14.

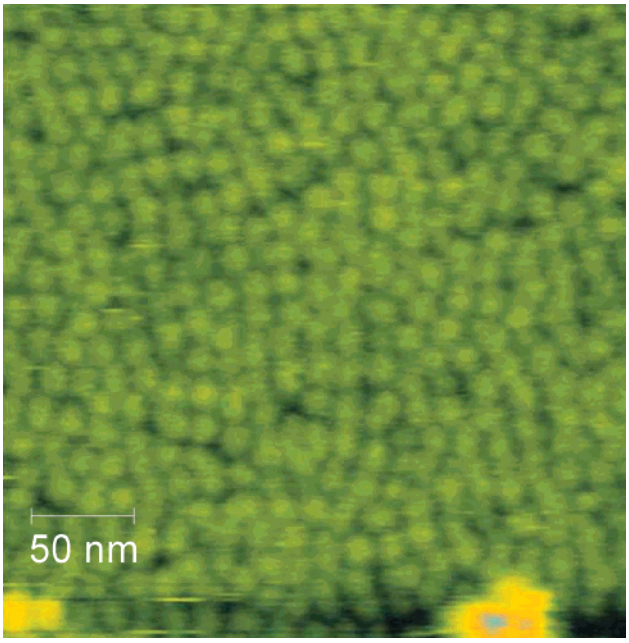

Figure 1. The surface of the glass bottom of the AFM cell in contact with a solution containing 0.23 mg mL^{-1} of apoferritin (supersaturation for crystallization $\sigma \equiv \Delta\mu/k_BT = 2.3$).

Results

Clusters on the Cell Bottom. Looking for molecular clusters, we monitored a bottom of the AFM cell prior to the formation of crystals. When the bottom was made out of silane-coated glass, it was covered by a thick disordered protein layer. Molecular resolution imaging of this layer was not possible, presumably because of the loose indirect attachment of the molecules to the bottom. As a next step, we tried uncoated glass: we used 12 mm diameter disks cut out of microscope cover slips (Corning, No. 2). At all protein concentrations tested, this substrate was fully covered by a monomolecular layer, Figure 1. This layer thickness was determined by intentionally pushing away[12] a few molecules and detecting the glass substrate in the void. Although each molecule has roughly hexagonal coordination within the layer, the layer is disordered and represents a two-dimensional glasslike phase. We never saw a full or partial second layer of adsorbed molecules. Continuous

(18) Hill, T. L. *Thermodynamics of small systems*; Benjamin: New York, 1963; Vol. 1.
(19) Petsev, D. N.; Vekilov, P. G. *Phys. Rev. Lett.* **2000**, *84*, 1339−1342.
(20) Petsev, D. N.; Thomas, B. R.; Yau, S.-T.; Vekilov, P. G. *Biophys. J.* **2000**, *78*, 2060−2069.
(21) Steinrauf, L. K. *Acta Crystallogr.* **1959**, *12*, 77−78.
(22) Atkins, P. *Physical Chemistry*, 6th ed.; Freeman: New York, 1998.
(23) Theil, E. C. *Ann. Rev. Biochem.* **1987**, *26*, 289−315.
(24) Lawson, D. M.; Artymiuk, P. J.; Yewdall, S. J.; Smith, J. M. A.; Livingstone, J. C.; Trefry, A.; Luzzago, A.; Levi, S.; Arosio, P.; Cesareni, G.; Thomas, C. D.; Shaw, W. V.; Harrison, P. M. *Nature* **1991**, *349*, 541−544.
(25) Hempstead, P. D.; Yewdall, S. J.; Fernie, A. R.; Lawson, D. M.; Artymiuk, P. J.; Rice, D. W.; Ford, G. C.; Harrison, P. M. *J. Mol. Biol* **1997**, *268*, 424−448.
(26) Thomas, B. R.; Carter, D.; Rosenberger, F. *J. Cryst. Growth* **1997**, *187*, 499−510.
(27) Yau, S.-T.; Vekilov, P. G. *Nature* **2000**, *406*, 494−497.
(28) Petsev, D. N.; Thomas, B. R.; Yau, S.-T.; Tsekova, D.; Nanev, C.; Wilson, W. W.; Vekilov, P. G. *J. Cryst. Growth*. **2001**, in print in the Proceedings of ICCBM-8.
(29) Hansma, P. K.; Cleveland, J. P.; Radmacher, M.; Walters, D. A.; Hillner, P.; Bezanilla, M.; Fritz, M.; Vie, D.; Hansma, H. G.; Prater, C. B.; Massie, J.; Fukunaga, L.; Gurley, J.; Elings, V. *Appl. Phys. Lett.* **1994**, *64*, 1738−1740.
(30) Noy, A.; Sanders, C. H.; Vezenov, D. V.; Wong, S. S.; Lieber, C. M. *Langmuir* **1998**, *14*, 1508−1511.

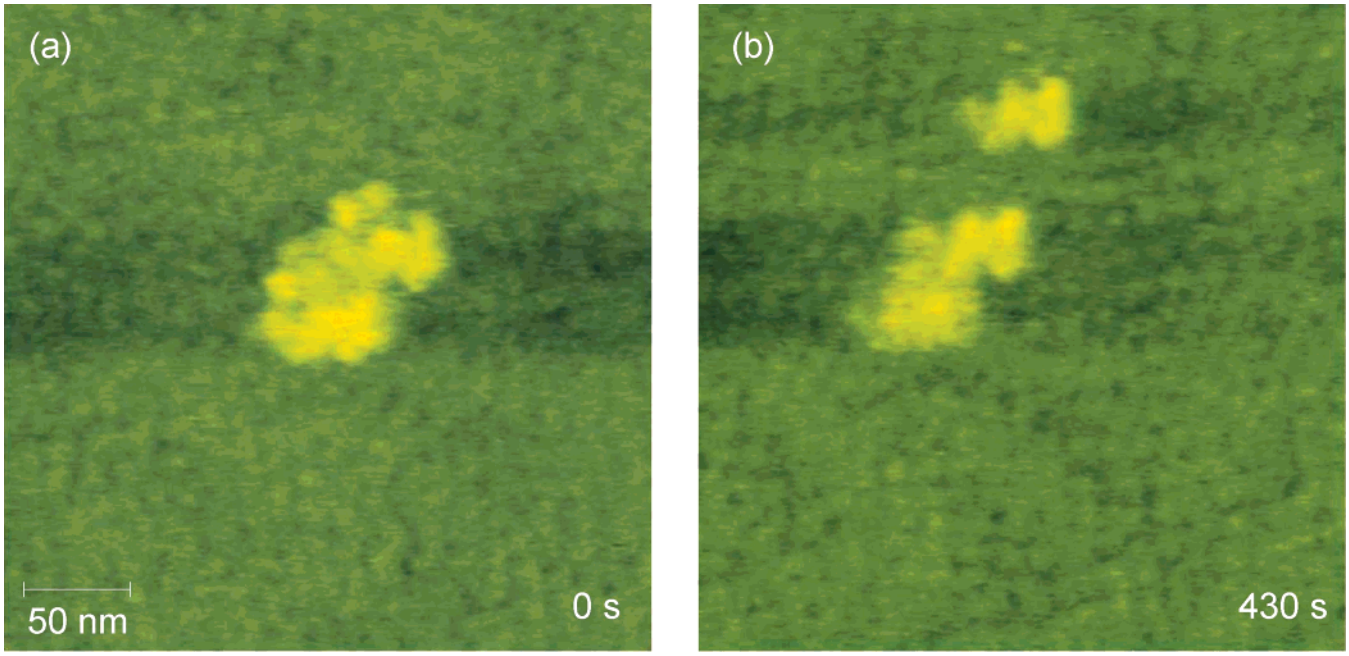

Figure 2. Landing of a cluster in the microscope viewfield on the glass bottom of the AFM cell. The solution contains 0.23 mg mL^{-1} of apoferritin (supersaturation $\sigma = 2.3$). Brighter yellow coloring corresponds to higher altitude: (a) a cluster consisting of about 20 molecules forming a single layer and (b) a second cluster of four or five molecules has landed in the viewfield. The cluster seen in part a has lost two molecules from the top and two from the left side.

monitoring for several hours showed no changes in the arrangements of the molecules and we conclude that the apoferritin molecules are rigidly attached to the glass substrate. This firm attachment allows imaging of single molecules and determination of their size of ~13 nm, the same as in a crystal,[12] and excludes the possibility that the clusters discussed below form on the bottom after rearrangement of the adsorbed molecules.

Initial scan widths were 2 to 10 μm. Figure 2 shows an example of a cluster containing four molecules landing near another one, which lost five molecules, two from its top and three form its left, during the monitored period. To obtain these images, after the landing of a cluster was detected, we zoomed in on it using scan widths of 1000 nm or less. Other examples of clusters consisting of 2, 4, 6, ~16, and ~20 molecules are shown in Figure 3. Typically, the clusters stay adsorbed for 2 to 30 min and then dissolve or desorb. Furthermore, in the smallest clusters, such as the top one in Figure 3a, the molecules occupy the corners of a polygon. Clusters of ~10−20 molecules consist of two parallel molecular rows, similar to the six-molecule cluster in Figure 3b. Quantifications of the vertical coordinate of the images, using the standard module of the Nanoscope IIIa software package, revealed that all clusters, such as those in Figure 3, parts c and d, consist of a single layer of molecules, with some molecules positioned higher than others.

These observations are insufficient to assign the clusters to the nucleation pathway of apoferritin crystallization. However, after we have discussed all available evidence about the nucleation process in this system, we will revisit them and show that these are subcritical clusters that constitute the early stages in the nucleation process.

Structures and Sizes of Near-Critical Clusters. The images of the molecules within the clusters in Figures 2 and 3 are fuzzier than those of the molecules in the underlying adsorbed layer in Figure 1. We attribute the lower clarity of the imaging to looser attachment of the clusters to the layer of adsorbed molecules. A substrate with a periodic structure and a characteristic length scale equal to the size of the protein molecule, such as the (111) face of a large apoferritin crystal, may provide for a stronger attachment and better visibility of the clusters.

However, in supersaturated solutions crystals grow and deplete the solution layer surrounding them. To test if such concentration nonuniformity may affect the cluster evolution, we performed numerical simulations of combined buoyancy-driven convection and solute diffusion.[31] At the average rate of growth of the underlying crystal of <0.1 nm s^{-1}, typical for the conditions used,[12] the characteristic diffusion and convection velocities are respectively 0.3 μm s^{-1} and <1 μm s^{-1}, and the apoferritin depletion at the interface is <1% (H. Lin, unpublished results). Such low depletion levels cannot significantly affect the nucleation process. Furthermore, the AFM tip travel for scan widths of 0.5 μm and frequencies of ~3 Hz and the ~20 kHz tapping oscillation could add solution flow with similar velocities and should not increase or decrease the depletion of the solution adjacent to the crystal.

While monitoring the surfaces of large crystals, we saw more than 20 events of cluster landing; representative examples are shown in Figure 4a,b. In all cases, the molecules in a cluster are arranged in rods of 4−8 molecules and the rods are assembled in domains of 3−7 rods in a plane with additional 2−3 rods forming a second layer. The cluster in Figure 4a contains two domains linked by a longer rod of about 10 molecules. The center-to-center distance between adjacent molecules in a rod is 13 nm, equal to that along the close-packed ⟨110⟩ direction in the crystal lattice. Furthermore, one of the molecular rows of the cluster in Figure 4b generates a new (111) crystal layer that spreads on the crystal surface to meet the crystal's own layer. We conclude that these are clusters of apoferritin molecules, which, unlike occurrences in other systems,[32,33] have the same arrangement as in the crystal.

(31) Lin, H.; Petsev, D. N.; Yau, S.-T.; Thomas, B. R.; Vekilov, P. G. *Cryst. Growth . Design* **2001**, *1*, 73−79.

(32) Kuznetsov, Y. G.; Malkin, A. J.; McPherson, A. *Phys. Rev. B* **1998**, *58*, 6097−6103.

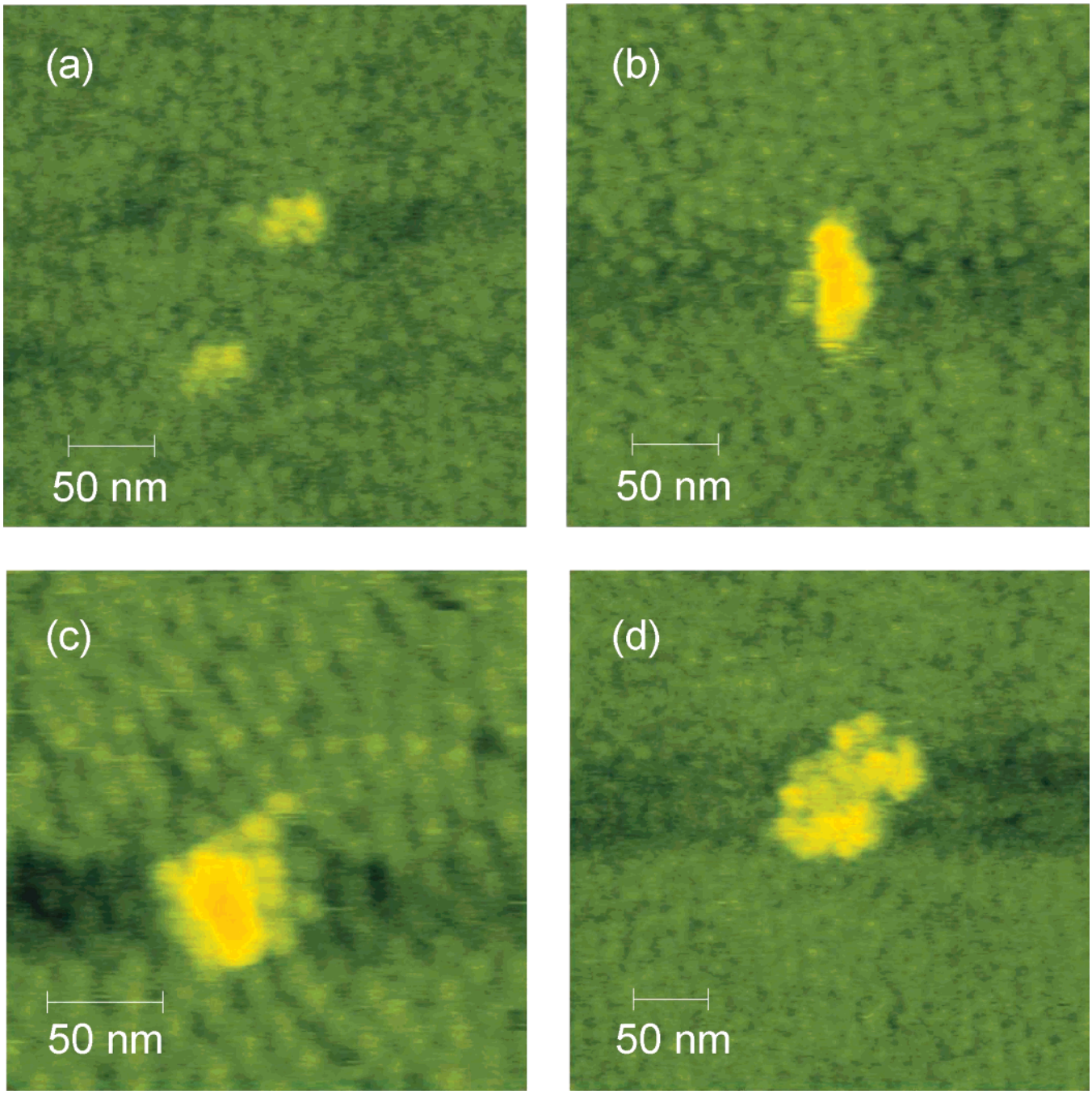

Figure 3. Examples of clusters seen on the glass bottom of the AFM cell at various protein solution concentrations and supersaturations. Brighter yellow coloring corresponds to higher altitude: (a) apoferritin concentration $C = 0.23$ mg mL^{-1}, supersaturation $\sigma = 2.3$, two clusters consisting respectively of two and four or five molecules; (b) $C = 0.04$ mg mL^{-1}, $\sigma = 0.5$, a cluster consisting of six molecules in two rods with four and two molecules in each of the rods; (c) $C = 0.046$ mg mL^{-1}, $\sigma = 0.7$, a flat cluster consisting of ~15−16 molecules; and (d) $C = 0.23$ mg mL^{-1}, $\sigma = 2.3$, a flat cluster consisting of ~20 molecules.

The quasiplanar shape of all seen clusters and the similarity to the shapes of the clusters seen on the glass bottom in the absence of crystals in the cell exclude the possibility that the clusters are pieces that break off a large crystal to land in our field of view. To further support the observation that the clusters were formed in the solution bulk and then landed on the monitored surface, we note that (i) the clusters do not consist of closely packed (111) planes, but of (110) planes, see Figure 4c. On the other hand, if nucleation occurs on the crystal surface, it produces nuclei of a new crystal layer that exactly replicate the (111) molecular arrangement of the underlying crystal layer.[12] (ii) The molecular rows in the cluster in Figure 4a are at an angle with the crystal's ⟨110⟩ direction. (iii) The cluster and the layer originating from it in Figure 4b are out of registry with the crystal's own layer causing a boundary free of molecules or consisting of strained molecules.

Dynamics and Long-Term Evolution. An example of the typical dynamics of the exchange of molecules between the clusters and solution is shown in Figure 5. We see that molecules attach to and detach from the cluster between two frames. The attachment and detachment frequencies are comparable, which is unusual for the supersaturated conditions of the observation.

(33) Georgalis, Y.; Umbach, P.; Raptis, J.; Saenger, W. *Acta Crystallogr. Sect. D* **1997**, *53*, 691−702.

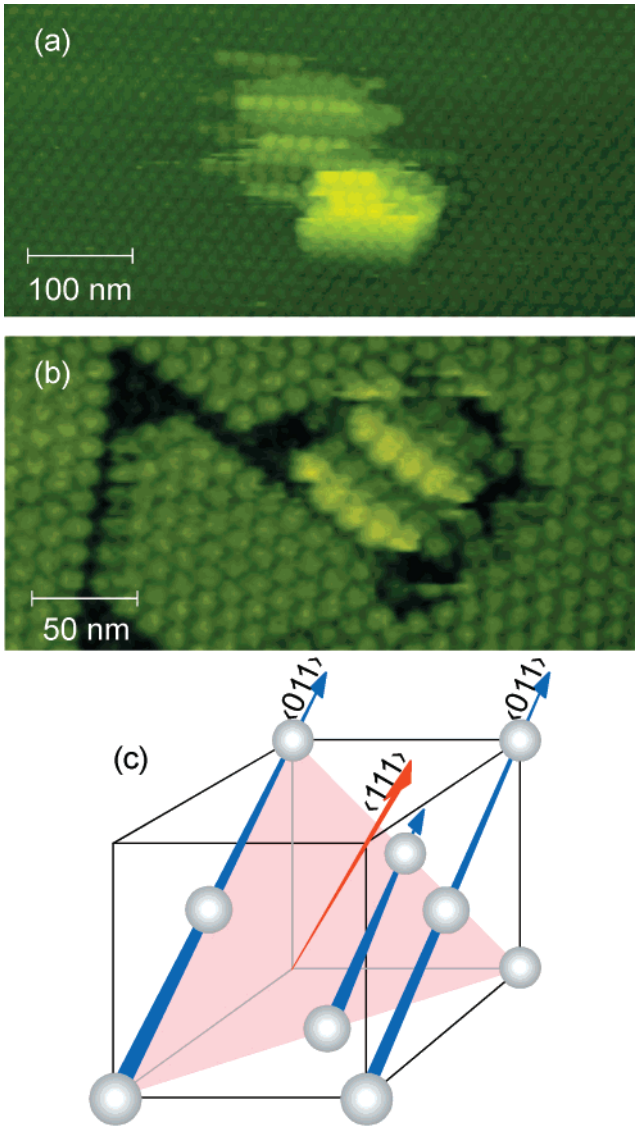

Figure 4. Near-critical clusters on the (111) face of an apoferritin crystal. Brighter yellow coloring codes are for higher altitude: (a) $C = 0.07$ mg mL^{-1}, $\sigma = 1.1$, the dark-green beehive pattern in the background is the (111) face of the apoferritin crystal used as a substrate. A cluster, in yellow, consisting of two domains; the upper domain consist of six or seven rods of four to seven molecules in each. The rods are parallel and positioned alternatively higher and lower in a harmonica pattern, in an arrangement corresponding to a (110) crystal layer, see part c. (b) $C = 0.115$ mg mL^{-1}, $\sigma = 1.6$. s. A cluster, consisting of four or five rods in a harmonica arrangement typical for the (110) layer of the apoferritin crystals, is surrounded on three sides by a layer of the underlying crystal formed after landing. Each rod has four to six molecules. The lower left rod of the cluster has initiated an island parallel to the crystal (111) planes. The molecules in this island are horizontally shifted from the crystallographic positions of the underlying crystal, resulting in a misfit boundary around the cluster and the island. (c) Schematic of (111), in pink, and (110), consisting of blue ⟨011⟩ rows, planes, and ⟨110⟩ molecular rows in a face-centered cubic (fcc) crystal lattice.

Estimating the average net frequency of molecular attachment and detachment in Figure 5, we get ~4 molecules/43 s ≅ 0.1 s^{-1} for the ~20 possible attachment sites at the ends of the molecular rows, or 0.005 s^{-1} per attachment site. This frequency is more than an order of magnitude lower than the net frequency of attachment to a growth site on the surface of large crystals, which is of 0.065 s^{-1} (ref 12) and is reflected in the fast motion

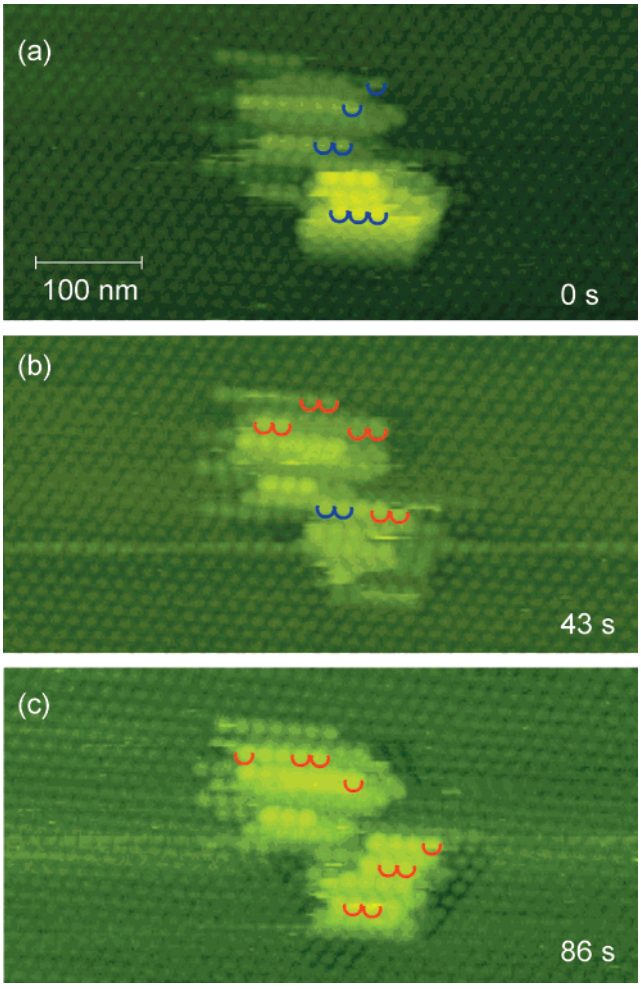

Figure 5. Dynamics of exchange between the cluster in Figure 4a and the solution with $C = 0.07$ mg mL^{-1}, $\sigma = 1.1$. (a−c) Molecules attach and detach from the cluster; molecules that are missing in the next frame are highlighted in blue, those that have appeared after the previous frame was captured are shown in red.

of the growth step seen in Figure 6. The low net exchange rate of the cluster with the solution suggests that the size of the cluster in Figure 5 is just above the critical size.

The cluster in Figure 7 loses one layer of 6 molecules for 896 s, compare parts a nad c in Figure 7. Hence, its size must be just below the critical size for that supersaturation. Similarly comparable rates of molecular attachment and detachmen, and bifurcation of subsequent evolution of the clusters into either growth or dissolution were observed for all clusters of such sizes seen in the experiments. We conclude that these are near-critical clusters for the phase transformation occurring in the system, crystallization of apoferritin. Their sizes are respectively slightly larger or smaller than the critical, and their structure should be representative of the structure of the nucleus.

A comparison of the sizes of the clusters in Figure 4 further supports this conclusion. The near-critical cluster in Figure 4a at $\sigma = 1.6$ is smaller than the one in Figure 4b at $\sigma = 1.1$. On the average, smaller near-critical clusters were observed at higher supersaturations. Although we do not have sufficient statistics for a quantitative statement, these observations agree with the predictions of the classical and advanced treatments of nucleation.[2,3,34]

(34) Mutaftschiev, B. In *Handbook of crystal growth*; Hurle, D. T. J., Ed.; Elsevier: Amsterdam, 1993; Vol. I, pp 189−247.

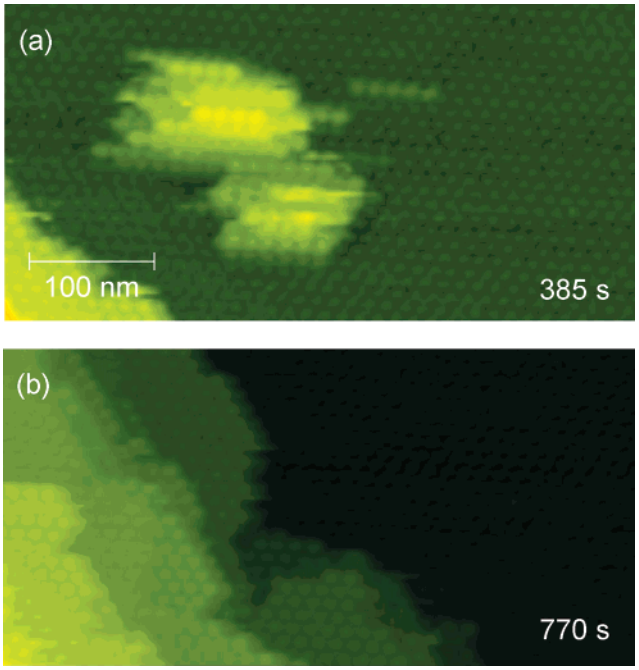

Figure 6. Long-term evolution of a cluster adsorbed on large crystals at $C = 0.07$ mg mL^{-1}, $\sigma = 1.1$. Same cluster as in Figure 5. Shown times are after the image in Figure 5a was recorded. (a and b) An advancing step pushes the cluster back into the solution. Note that (i) the step velocity is 0.6 nm/s, close to the fastest step velocity previously recorded for this supersaturation with apoferritin crystals,[12] and (ii) the cluster in part a is significantly larger than that in Figure 5c, in agreement with the trend of more attachment than detachment events in Figure 5. There were several pauses in imaging of up to 5 min between the collection of the images shown in Figures 5 and 6. Observations i and ii indicate that the selected AFM imaging mode did not affect the monitored processes.

Did the cluster structure change after landing? To address this question, we monitored the long-term evolution of the near-critical clusters. We see that some of them are pushed back into the solution by the advancing crystal layers similar to the cluster in Figure 6. Some of the clusters, an example is shown in Figure 7, are trapped by the crystal layers. In such cases, as illustrated by Figure 7d, a misfit boundary between the two structures always appears, similar to the misfit boundaries forming upon incorporation of larger crystallites discussed in detail in refs 35 and 36. If the cluster shape had changed, we would expect continuity between the cluster and the underlying crystal, similar to observations of landing droplets of high-density protein solution in refs 32 and 37. Hence, we conclude that the clusters form in the solution and do not change their shape upon landing.

Behavior of Individual Subcritical and Near-Critical Clusters. Figure 8a shows two clusters adsorbed on the protein-covered surface of the AFM cell bottom at $C = 0.23$ mg mL^{-1} and supersaturation $\sigma = 2.3$. The smaller cluster contains four molecules, while the larger one contains nine molecules. The scaling laws, discussed below, suggest that the larger cluster's size is close to the critical size for that supersaturation. Correspondingly, the smaller cluster is significantly smaller than the critical size. From the predictions of the nucleation theories,[34] we would expect the smaller cluster to quickly disappear, while the larger one could be close to a labile equilibrium with the solution. However, parts b−d in Figure 8 reveal that the smaller cluster receives and loses two molecules, remaining with four molecules at the end of the ~20 min monitoring, while the larger cluster systematically dissolves over the same time period. This seeming contradiction is resolved by the realization that the nucleation theories describe the evolution of large populations of clusters. The fate of individual clusters is determined by a random sequence of events and can be random itself.

These observations may have implications for the understanding and prediction of the behavior of ensembles of small aggregates undergoing surface energy-driven Oswald ripening that form the basis of many recent nanotechnologies.[38]

Do These Clusters Evolve Into Crystals? Figure 9 shows that the clusters that form in the solution may develop into (111) facetted fcc crystals. We see a microcrystal that consists of three (111) layers of about 60 molecules in each. The microcrystal is inclined with respect to the substrate by about 3°, Figure 9d. This corresponds to one molecule trapped under the microcrystal close to its edge or to an unfinished layer on its bottom surface. The inclination suggests that the microcrystal formed in the solution bulk and later landed on the viewed crystal surface. Clusters similar to those shown in Figures 4−7 can evolve to such a microcrystal by accumulating several (110) layers until a (111) face is formed.

Discussion

The nucleation pathway emerging from the above observations is schematically summarized in Figure 10. For Stage I, single molecules in the solution, the lack of any significant concentration of labile dimers, trimers, etc. has been evidenced by dynamic light scattering.[20] Stage II, a few molecules at the corners of a polygon, corresponds to clusters in Figures 2, 3a, and 8. Stage III represents a linear array as in Figure 3b. Stage IV is a quasiplanar critical cluster with (110) orientation, similar to structures seen in Figures 4−7. During Stage V, microcrystal facetted by (111) planes as in Figure 9, the (110) layers stack up to form this crystal.

Although the arrangement of the molecules in the nuclei is similar to that in the crystal, the (110) planar structure of the nucleus is surprising: one would expect a cluster of four or more quasispherical apoferritin molecules to be a compact three-dimensional formation as shown in Figure 4b.[5,6] At this point, in analogy to the case of anisotropic dipolar molecules,[9] we can speculate that the slight anisotropy of the apoferritin molecules, either directly or after enhancement by the formation of a two-member cluster, underlies the observed shape. Another possible mechanism underlying this shape may be related to rotational relaxation of the molecules in the top crystal layer evidenced in ref 14. A correlation between some types of surface relaxation in crystals and a planar shape of the clusters whose size is in the region of surface energy-controlled morphology has been predicted.[10]

This nucleus structure may have drastic consequences for the nucleation process. A planar cluster has larger surface area than a compact cluster with the same number of molecules n. As a

(35) Malkin, A. J.; Kuznetsov, Y. G.; McPherson, A. *J. Struct. Biol.* **1996**, *117*, 124−137.
(36) Malkin, A. J.; Kuznetsov, Y. G.; McPherson, A. *Proteins: Struct. Funct. Genet.* **1996**, *24*, 247−252.
(37) Kuznetsov, Y. G.; Malkin, A. J.; McPherson, A. *J. Cryst. Growth* **1999**, *196*, 489−502.
(38) Morgenstern, K.; Laegsgard, E.; Stensgaard, I.; Basenbacher, F. *Phys. Rev. Lett.* **1999**, *83*, 1613−1619.

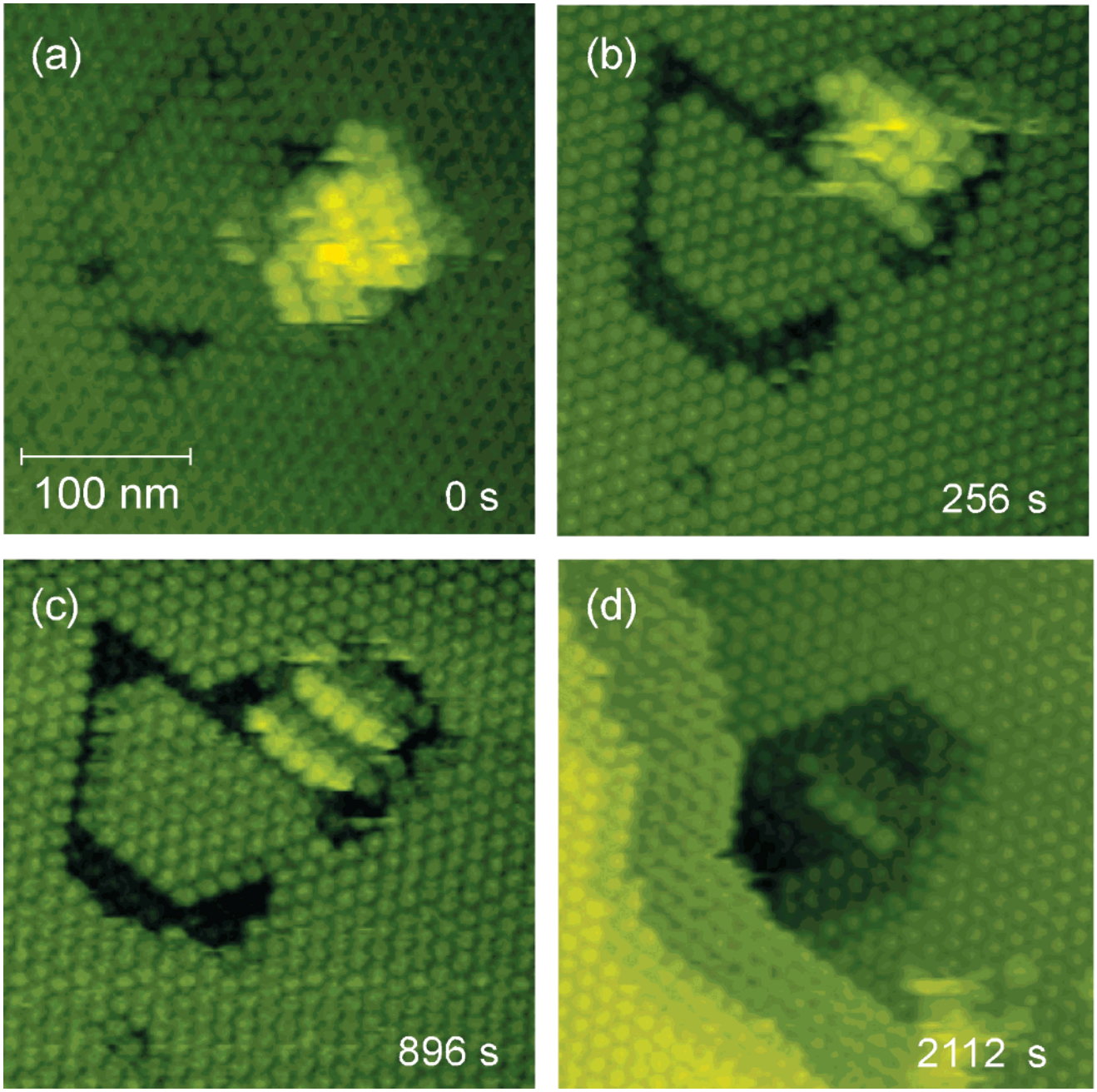

Figure 7. Slow dissolution of the cluster in Figure 4b at $C = 0.115$ mg mL^{-1}, $\sigma = 1.6$. (a−c) The top layer of the cluster is gradually disappearing because more molecules detach than attach to the cluster. The fraction of the top crystal layer originating from the cluster is out of registry with the underlying crystal. (d) A few steps belonging to the crystal surround the cluster—note the misfit between the molecules of the crystal and those of the cluster. The direction of scanning was changed between parts a and b. The consistency of the cluster structure evidences the lack of AFM imaging artifacts.

result, a larger contribution to the crystallization energy gain is needed to compensate for the greater surface energy loss, and hence the number of molecules in the critical cluster n^* is greater. Since under quite general assumptions $\Delta G(n^*) = n^*\Delta\mu/2$,[39,40] this leads to higher nucleation barriers and slower nucleation kinetics than predicted by the classical theories that assume compact spherical clusters. Furthermore, the rough surface of the nuclei in Figures 4−7 may result in the surface energy that is not a smooth or monotonic function of the nucleus size. This may result in rather unusual dependencies of the nucleation rate on $\Delta\mu$.

Next, we tested if the observed cluster shapes and sizes are consistent with the available data on apoferritin and its crystallization. For a crude quantification of the nucleation process, we approximate the critical cluster with a square of one or two crystalline layers, with n_e molecules on its edge. The labile equilibrium of the critical cluster with the medium represented as IV in Figure 10a is around states in which the second layer is being built. To calculate the average reversible work per molecule $\Delta G/\Delta n$, $\Delta n = n_e \times n_e$, needed to build the second layer, we follow the logic of refs 41−43. At constant temperature and pressure, $\Delta G/\Delta n$ for the addition of a (110) layer

(39) Kashchiev, D. *J. Chem. Phys.* **1982**, *76*, 5098−5102.
(40) Oxtoby, D. W.; Kashchiev, D. *J. Chem. Phys.* **1994**, *100*, 7665−7671.
(41) Stranski, I. N.; Kaischew, R. *Z. Phys. Chem* **1934**, *B26*, 100−113.
(42) Stranski, I. N.; Kaischew, R. *Z. Phys. Chem* **1934**, *B26*, 114−116.
(43) Kaischew, R.; Stranski, I. N. *Z. Phys. Chem* **1937**, *B35*, 427−432.

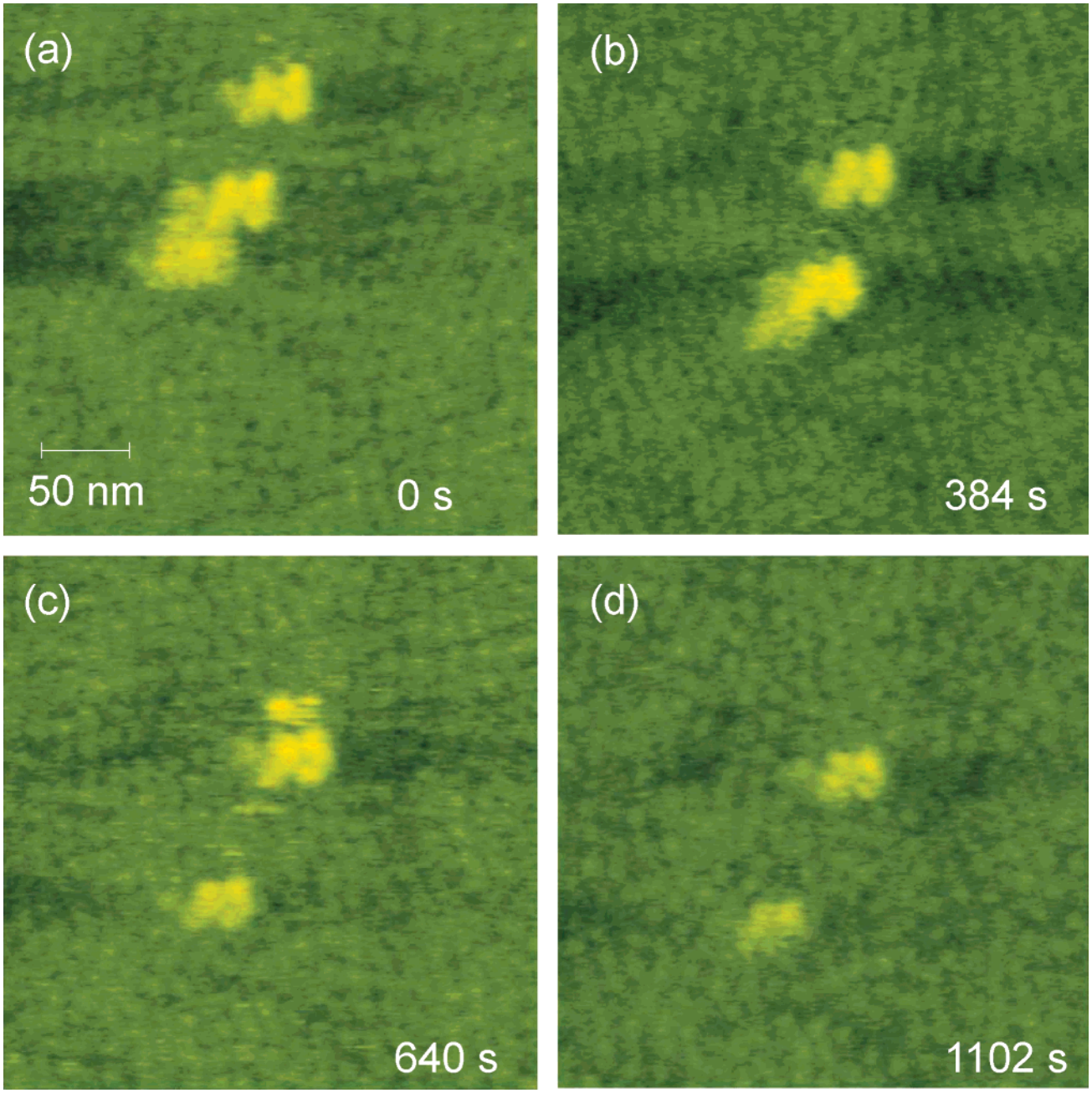

Figure 8. (a−d) Evolution of two clusters adsorbed on the glass bottom of the AFM cell at protein solution concentrations of $C = 0.23$ mg mL^{-1} and supersaturation $\sigma = 2.3$.

consisting of $n_e \times n_e$ molecules to a (110) surface is

$$\frac{1}{n_e^2}(6n_e^2\phi - 2n_e\phi) = 6\phi - \frac{2\phi}{n_e} \qquad (1)$$

Here ϕ is the free energy of formation of one intermolecular bond from solute molecule (the entropic components mostly stem from the waters trapped in the crystal or bound to the solute[14]). The sum in eq 1 contains the work to add $(n_e - 1)^2$ molecules to kinks on (110) surfaces by forming alternatively 8 or 4 bonds with neighbors from the new and the lower layers, $2(n_e - 1)$ molecules along the edges of the layer that are bound to 5 or 3 molecules, and one molecule bound to three or one molecule from the lower (110) layer. Ignoring the crystallization entropy change due to the protein molecules (significantly smaller than the contribution of the water molecules[14,44]), the first term on the right side of eq 1 is the average change of free energy upon crystallization per molecule, i.e., $\Delta\mu$. The second term is the excess free energy of the cluster surface. For a critical cluster in labile equilibrium with the solution, the difference in eq 1 equals zero, and the Gibbs−Thomson equation obtains[41−43]

$$\Delta\mu = 2\phi/n_e \qquad (2)$$

Monitoring the dynamics of molecular incorporation on the (111) apoferritin surface, we obtained for ϕ values of $\phi/k_BT = 3.2$.[12] In ref 14 we have shown that this value of the free energy of formation of one intermolecular bond is in good agreement with the free energy for crystallization, determined from

(44) Israelachvili, J. N. *Intermolecular and Surface Forces*; Academic Press: New York, 1995.

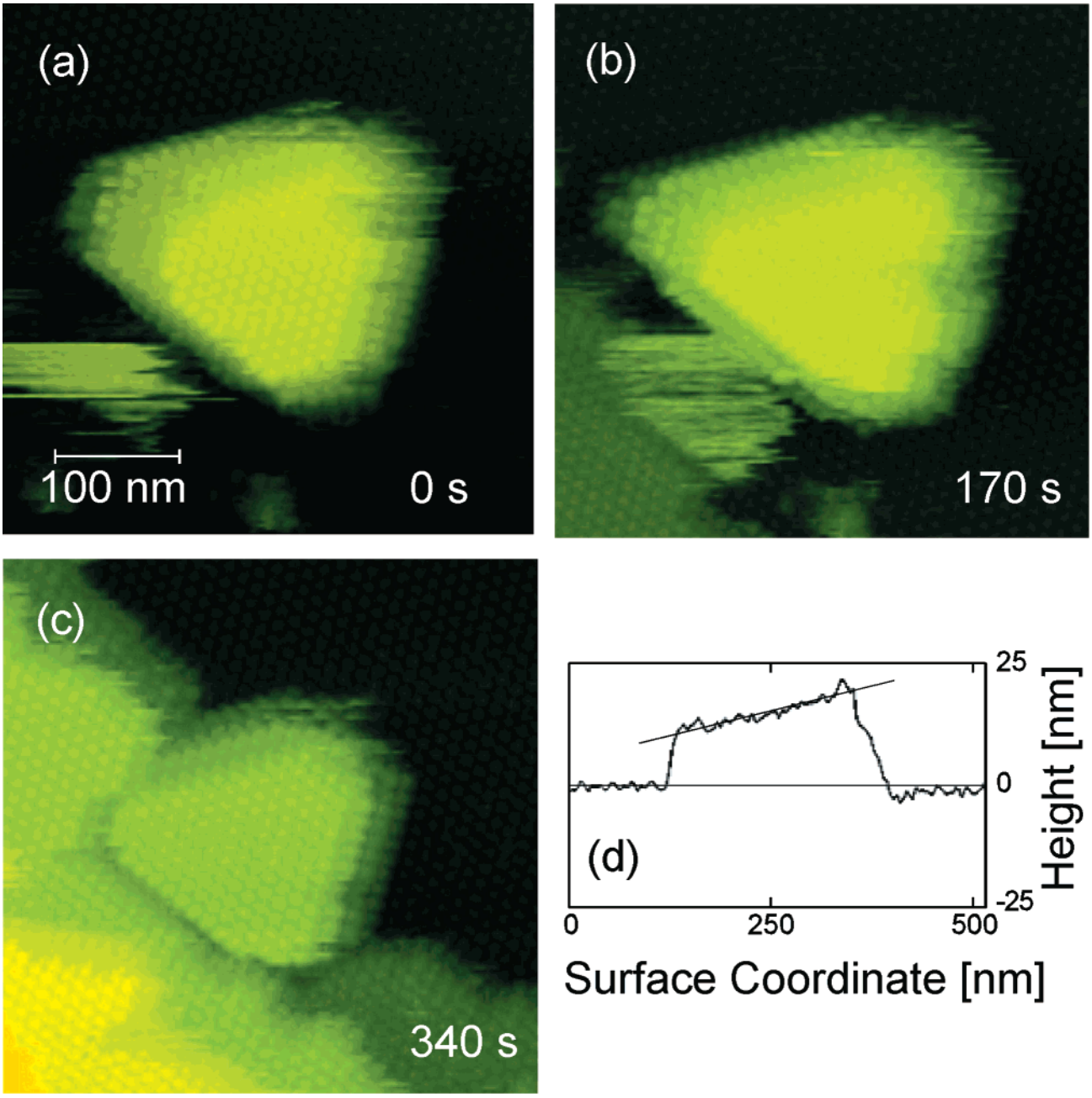

Figure 9. Microcrystal landing on a large crystal at $\sigma = 1.1$. (a−c) The microcrystal slowly grows by attachment of molecules to the side (110) faces, while a step belonging to the underlying crystal rushes forward to incorporate it. (d) The height profile along a line roughly from top left to bottom right in part a.

solubility data. Substituting in eq 2, we find that with the supersaturations for the clusters in Figure 4, $\sigma \equiv \Delta\mu/k_BT = 1.1$ and 1.6, the values of n_e are 6 and 4, respectively. These are close to the actual sizes of clusters at these supersaturations. Hence, ϕ is the molecular-level equivalent to surface tension that governs nucleation.[41−43]

Comparing the n_e's with the respective n^*'s, at $\sigma = 1.1$, $n^* \approx 60$ (Figure 5) and at $\sigma = 1.6$, $n^* \approx 25$ (Figure 7), we find that

$$n^* \approx n_e^{2.3} \qquad (3)$$

The exponent linking n^* and n_e is between 2, corresponding to a planar cluster, and 3, corresponding to a compact three-dimensional cluster. Extrapolating to $C = 1$ mg mL^{-1}, $\sigma = 3.8$, at which apoferritin crystals are typically grown,[26] we get $n_e \approx 1$ or 2, $n^* \approx 3-4$ (for structures of such clusters imaged by AFM at lower σ's, see Figure 3). Assuming a preexponential factor for the nucleation rate law $J_0 \sim 1$ cm^{-3} s^{-1} (for lysozyme, J_0 is between 1 and 10 cm^{-3} s^{-1} refs 45−48) and using, as above, $\Delta G^* = n^*\Delta\mu/2$, we get for the nucleation rate $J = J_0 \exp[-\Delta G^*(n^*)/k_BT] \approx 10^{-3}$ cm^{-3} s^{-1}. In an overnight experiment with a few hundred microliters of solution, ~10 crystals should nucleate. Accordingly, numerous experiments under these conditions produced between a few and ~100 crystals.

To compare the estimated ϕ to previous results, we define a corresponding effective macroscopic surface energy γ as

(45) Vekilov, P. G.; Monaco, L. A.; Thomas, B. R.; Stojanoff, V.; Rosenberger, F. *Acta Crystallogr. Sect. D* **1996**, *52*, 785−798.
(46) Galkin, O.; Vekilov, P. G. *J. Phys. Chem.* **1999**, *103*, 10965−10971.
(47) Galkin, O.; Vekilov, P. G. *J. Am. Chem. Soc.* **2000**, *122*, 156−163.
(48) Galkin, O.; Vekilov, P. G. *Proc. Natl. Acad. Sci. U.S.A.* **2000**, *97*, 6277−6281.

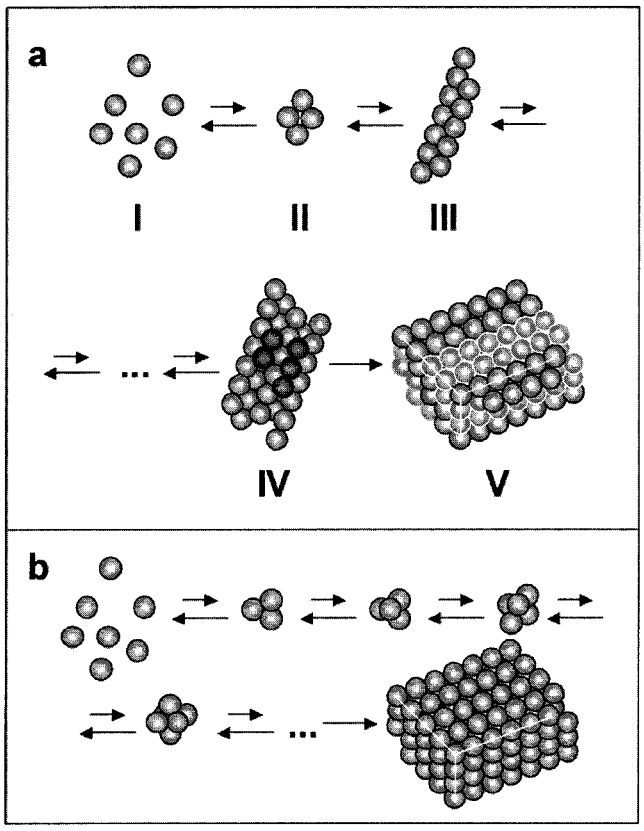

Figure 10. Schematic illustration of two nucleation pathways: (a) via a planar critical cluster (in IV molecules belonging to the second layer are shown in a lighter shade; in V the (110) layers that stack up to form this crystal are delineated by lighter and darker contours) and (b) via compact critical cluster.[5,6]

$n_{free}\phi/S$. Here n_{free} is the number of unsaturated bonds of a molecule on the surface of a nucleus, and S is the surface area of a molecule. With n_{free} on the average of 7−8 for the clusters that expose two sides of many molecules, see Figure 4, we get $\gamma \approx 0.2$ mJ m^{-2}. Light-scattering determinations of apoferritin nuclei sizes averaged over all body angles[49] at $\sigma = 0.92$ yielded values of ∼40 nm (or ∼3.5 molecular dimensions, compatible with the cluster in Figure 4a). Assuming spherical nucleus shape, the authors obtained $\gamma = 0.027$ mJ m^{-2}.[49] As discussed above, the surface energy should be lower for a spherical than for a flat cluster. Likely, this underlies the lower estimate of γ. Similarly, AFM studies of virus crystallization kinetics[50] produced γ-values higher by about the same factor than the evaluation based on light scattering.[49]

Conclusions

Our results for the protein apoferritin show that (i) the arrangement of the molecules in the new-phase nuclei is similar to that in the crystal and (ii) the nucleus shape can differ from the generally accepted shape even for quasispherical molecules such as apoferritin. The second fact could lead to significant deviations of the thermodynamics and kinetics of nucleation of first-order phase transitions from those predicted by the existing nucleation theories. Similarly unexpected nuclei structures might be common. Hence, the nucleus structure should be considered as a variable by advanced theoretical treatments. The reasons underlying the observed nucleus shape, as well as possible other nuclei shapes, merit detailed theoretical and experimental studies.

Acknowledgment. We thank D. W. Oxtoby, D. Petsev, and O. Galkin for suggestions and constructive criticisms of various aspects of this work and H. Lin for access to unpublished modeling results. Research support by the National Heart, Lung, and Blood Institute, NIH (Grant HL 58038), the Life and Microgravity Sciences and Applications Division of NASA (Grants NAG8 1354 and 97 HEDS-02-50), and the State of Alabama through the Center for Microgravity and Materials Research at the University of Alabama in Huntsville is gratefully acknowledged.

JA003039C

(49) Malkin, A. J.; McPherson, A. *Acta Crystallogr. Sect. D* **1994**, *50*, 385−395.

(50) Malkin, A. J.; Land, T. A.; Kuznetsov, Yu. G.; McPherson, A.; DeYoreo, J. J. *Phys. Rev. Lett.* **1995**, *75*, 2778−2781.